



Research Into the Metal/Metalloid Movements in Soil and Groundwater in the Areas Surrounding the Coal Waste Dump Hałda Ruda (Upper Silesia, Poland)

Magdalena Jabłońska-Czapla^{}, Czesława Rosik-Dulewska^{*},
Sebastian Szopa^{*}, Piotr Zerzucha^{**}*

^{}Institute of Environmental Engineering PAS, Zabrze*

*^{**}University of Silesia*

1. Introduction

Upper Silesia is highly degraded due to the anthropogenic activity. On the one hand, the industrialization facilitated the economic development of the Upper Silesian cities. On the other hand, it caused serious environmental pollution [3, 21]. Many highly urbanized and industrialized cities in Upper Silesia do not possess data on the degradation level of the surface ground or dynamics of negative phenomena. Moreover, there is no assessment of the ground transformation under severe anthropopressure conditions. Determining the influence of changes in the environment resulting from its exploitation is still an important matter [6, 7, 10, 16], particularly in degraded areas, such as those in Upper Silesia.

Heavy metals are the main soil pollutants. They pass into groundwater and pollute the surrounding areas. Increased contents of heavy metals can adversely affect biological properties of soils. They may also contaminate ground and underground water and toxically influence the plants. Natural contents of heavy metals in soils do not usually pose a threat for plants, animals or humans. Unfortunately, the area of soils with the natural heavy metal contents gradually decreases due to the impact of human civilization and industrialization, which is confirmed by

many studies [36]. What is more, gaps in the knowledge of the natural heavy metal contents in soils usually result in oversimplifications in the assessments and interpretations of heavy metal pollution causes. Rock waste from hard coal mines is the main type of waste generated in Poland and stored in the dumps every year. Coal mine dumps ought to be perceived as serious and long-term sources of groundwater pollutants. The pollution potential of low-buffered capacity and acidification of waste increases with time because of FeS_2 decomposition [32].

Modern analytical methods, such as the EDXRF spectrometry and ICP-MS, enable simultaneous determinations of numerous analytes. They offer low limits of detection and high selectivity, which extends the research area. On the other hand, the amount of the obtained multidimensional data is massive. The information requires long-term analysis. Consequently, a number of problems related to the visualization and correct interpretation of the results arise. Chemometrics concerns the extraction of relevant information from measurements and chemical experiments through the effective organization of the analytical processes [5, 31]. Its tasks include experiment optimization, correct calibration, quality control and final data analysis. Chemometrics requires a proper definition of the problem, a detailed experiment plan and its realization carried out in accordance with the principles of the chemical metrology. Under such circumstances, chemometric analysis of the obtained results offer correct assessments and valid conclusions. The X-ray fluorescence (XRF) is one of the most popular methods used to examine elemental compositions of soils. The XRF meets the requirements for modern laboratory techniques [23]. It enables quick determinations of qualitative compositions. On the other hand, establishing precise quantitative compositions involves procedures of matrix effect correction, which entails a large number of standards [39]. At present, the Energy Dispersive X-Ray Fluorescence (EDXRF) is one of the best techniques for qualitative and quantitative analysis of heavy metals. It enables researchers to investigate concentrations of main and trace elements present in soils [4, 12, 20, 38], bottom sediments [2, 8, 18], ashes [9] or minerals [11, 22]. The EDXRF is a relatively simple and inexpensive method in comparison with other techniques for quantitative and qualitative analysis of metals.

At present, the inductively coupled plasma – mass spectrometry (ICP-MS) is the best method supporting researchers in quantitative analy-

sis of metals and metalloids at the ppt/ppb concentration levels. It is an appropriate tool for analyzing elements in a broad range of concentrations. Importantly, it is commonly used for the environmental analysis [14, 30].

The researched site lies in the north of the Silesian Upland, namely in the north-west part of the Bytom-Katowice Plateau. The morphological diversification of the area around the coal waste Hałda Ruda is not high. Its ordinates range between +251 m and +280 m AMSL. The coal waste dump is the local uplift dominating the surroundings (+270 m – 275 m AMSL). It lies in the catchment area of the Bytomka River, which is a tributary of the Kłodnica River, placed in the basin of the Oder. The Hałda Ruda is placed on the south bank of the Bytomka River, west of Ruda Śląska. The coal waste dump covers approx. 396,137 m². Its cubic capacity is 5,100,000 m³. It was opened in 1957 as a dump site of the *Zabrze-Bielszowice* coal mine, which is closed at present. The Hałda Ruda was planted with trees on its eastern side in the years 1963–1975. The northern slope was planted with trees from the Bytomka River side in the 1990s. The western part was partially reclaimed. Grass and bushes were planted with fly ashes and humus. Unfortunately, the unfinished reclamation resulted in the formation of extremely steep slopes. They are exposed to severe water and wind erosion which is increased due to the lack of the plant cover. The discussed part of the coal waste dump has been active thermally, which poses a threat to plants, animals, local inhabitants and people located at the dump. The rails from Katowice to Gliwice run south of the Hałda Ruda. Low residential buildings and allotments are situated along the neighboring *Szczęść Boże* Street. The area in which the coal waste dump is located is occupied by fields, fallow lands, meadows, parks and gardens. The southern and eastern parts are partially covered with trees. The climatic conditions of Zabrze are influenced by the local climate of the western part of the Upper Silesian Industrial Region. They are also modified by the city impact itself. The thickest cloud cover is observed in January. The annual cloudiness percentage varies between 0.6% and 2.9%. The average annual air temperature is +6.9°C. The average temperature values for January and July are -3.9°C and +17.5°C, respectively. The maximum precipitation is observed in July (87 mm), while the minimum is found for February (40 mm). The vegetation season lasts approx. 205 days. Zabrze is under the dominant influence of the southwest winds.

The aim of the following study was optimization and validation quantitative analysis metal(loid)s using EDXRF and ICP-MS technique to identify the pollutants occurring around the coal waste dump Hałda Ruda, which served as a storage site for waste from hard coal exploitation and processing. Its other purpose was to determine the way in which metals and metalloids moved in the surroundings of the dump site. The research was conducted to understand how the waste, stored over the years, influenced the changes in salinity and metal/metalloid concentrations in the soil and groundwater depending on the distance from the coal waste dump. It was also performed to recognize the impact of the waste on the characteristics of the soil and water environment. In the research process, total contents of metals and metalloids were determined in the soil samples with an EDXRF spectrometer. Groundwater samples were analyzed with an ICP-MS spectrometer. Additionally, the obtained results were analyzed chemometrically. The aim was to determine the correlations between the contents of particular elements, physicochemical conditions and the sampling site and genetic soil horizon of a given sample.

2. Materials and methods

2.1. Sampling

2.1.1. Soil samples

The soil was sampled at transects located at the sites shown in Figure 1. The groundwater runoff direction was taken into account during the sampling. The sampling points were situated at different distances from the coal waste dump to determine the range of the waste impact on the variations in metal concentrations in the soil samples. Specific transects were given the Roman numerals, whereas the sampling points were marked with the Arabic ones. The boreholes with the mounted piezometers were marked with the P8–P12 symbols. The soil pits were prepared at each sampling site. One was located on the groundwater runoff. The other one was placed on the groundwater inflow.

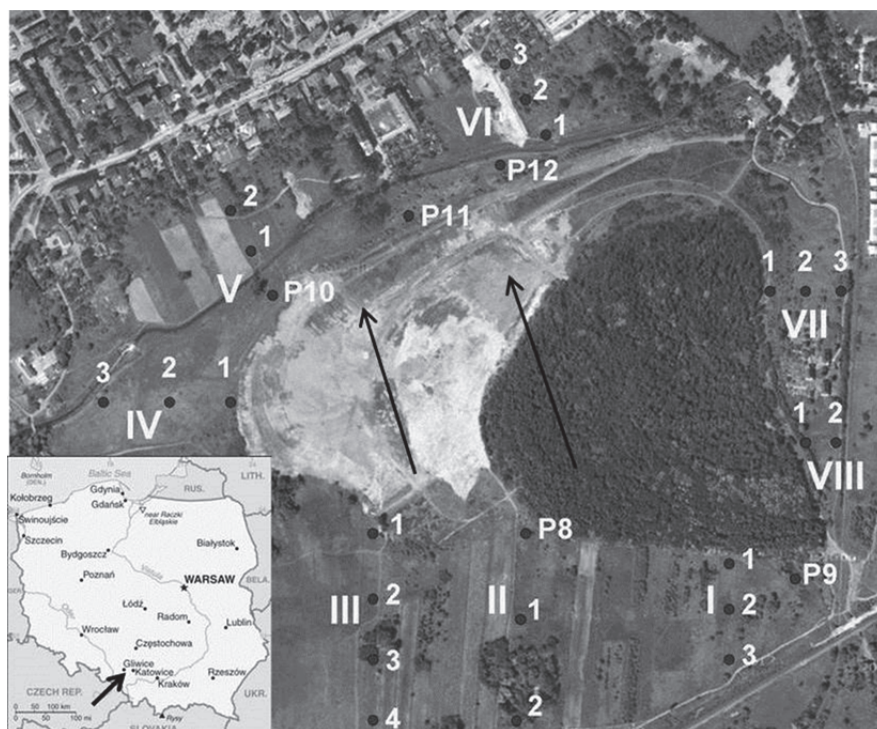


Fig. 1. Sampling sites at the Hałda Ruda: transects (I–VIII); sampling points (1–4); piezometers (P8–P12); arrows (groundwater runoff direction)

Rys. 1. Rozmieszczenie punktów poboru Hałda Ruda, I–VII transekty, 1–4 punkty poboru, P8–P12 piezometry, strzałki – kierunek spływu wód gruntowych

The soil sampling was performed with the borehole technique. The boreholes were made with manual tools equipped with Edelman drills (Eijkelpamp). They were drilled until the bedrock or aquifers were reached. The drilling was also stopped at the depth of 4 m (depth possible to reach with the drill set). Agricultural maps and several soil pits were used to determine the soil type and structural group. The soil was sampled at the sites where the owners had consented. The terrain could not be changed by agriculture and its morphology had to allow the drilling. Table 1 presents the distances of the sampling points from the coal waste dump and the borehole depth. The collected soil samples were averaged within the frame of a given genetic horizon in the field. The sample of a few kilograms was transported into the laboratory.

Table 1. Hałda Ruda sampling point locations and borehole depth
Tabela 1. Hałda Ruda odległości punktów poboru i głębokość odwiertu

Transect number	Sampling point number	Distance from the coal waste dump [m]	Borehole depth [cm]
I	1	10	80
	2	91	110
	3	180	235
II	P8	3	720
	1	89	250
	2	255	300
III	1	9	300
	2	114	190
	3	207	105
	4	310	300
IV	1	4	315
	2	117	300
	3	260	210
V	P10	18	1050
	1	71	300
	2	105	210
VI	1	27	100
	2	63	290
	3	97	200
VII	1	6	200
	2	53	160
	3	112	200
VIII	1	11	210
	2	59	245

2.1.2. Groundwater samples

Groundwater was sampled between 2010 and 2012. To do that, the piezometer network, created specifically for the project, was used. The piezometers were installed on the groundwater inflow and runoff in the examined area (Figure 1). The groundwater was sampled from the piezometers every month with the whistle, used to determine the water table level, and the Gigant water pump (max head: 20 m). The groundwater samples were always collected after the piezometers were emptied. After the piezometer was filled again, the water was collected into a 1-liter plastic container without the air access (the container was completely filled).

2.2. Sample preparation

The samples were dried in an electric dryer at 105°C for 90 minutes. Afterwards, they were sieved through a 2 mm sieve to remove any big objects (leaves, sticks, stones, etc.) from the samples. The obtained material was highly homogenous. It was dried again in the electric drier to obtain constant mass. The samples were ground in a vibratory grinder with the grinding vessel made of tungsten carbide (Testchem, Poland) for 2 minutes. For the analyses, carefully weighed amounts of standards or real samples (7.2 g) were mixed with the binder (0.8 g), i.e. synthetic wax (STW wax batch 64, PANalytical). Finally, the mixture was pressed with a manual hydraulic press (under the approx. 20 Mg pressure) for 2 minutes.

The groundwater samples were acidified with the ultrapure concentrated HNO₃ (Merck, Germany) and filtered through a 0.2 µm PES syringe filter immediately after they were transported into the laboratory. Afterwards, they were stored in a fridge at 2°C–5°C. Each sample was measured three times with the ICP-MS spectrometer.

2.3. Apparatus

Contents of the elements (Al, Si, K, Ca, Ti, V, Cr, Mn, Fe, Ni, Cu, Zn, As, Rb, Sr, Zr, Mo, Cd, Sb, Cs, Ba, Pb, Y, Nb, Sn, I, Bi) were determined in the soil using EDXRF spectrometer. A PANalytical Epsilon 5 was used for the measurement. The Epsilon 5 was equipped with a water-cooled X-ray tube with a side window (gadolinium anode; working range: 25 kV–100 kV; 150 µm beryllium window), a system of 9 secondary targets (Al, Ti, Fe, Ge, Zr, Mo, Ag, Ce₂O₃, Al₂O₃) and a Ge(Li) detector (resolution: 140 eV; energy range: 0.7 keV–100 keV; working surface: 30 mm²; 8 µm beryllium window). Due to the application of the 3-D optical path in the Epsilon 5, the dispersed radiation from the X-ray tube did not reach the detector and did not disturb and/or falsify the results. Instead, it disappeared because of the polarization. It demonstrated itself through the very low background in the spectrum. Coupling the apparatus with advanced software helped to determine the intensity of peaks, even very low ones. Consequently, it was possible to determine element concentrations in the investigated sample at extremely low levels. Certified reference materials for soils were used to calibrate the spectrometer. 40 certified reference materials were used to create the

calibration lines and two others were later used to verify the calibration and to establish factors such as repeatability, intermediate precision or recovery. The groundwater analyses were performed with an ICP-MS Elan DRC-e 6100 spectrometer (Perkin-Elmer). It was equipped with a standard ICP quartz torch, cross nebulizer and nickel cones. Samples and standards were fed with a peristaltic pump. The spectrometer was optimized to provide maximal intensity for ^{24}Mg , ^{115}In , ^{238}U , and minimal values for CeO/Ce (below 3%) and Ba $^{2+}$ /Ba (below 3%). A special application was prepared. It helped to measure the following isotopes: ^{51}V , ^{53}Cr , ^{55}Mn , ^{59}Co , ^{60}Ni , ^{65}Cu , ^{66}Zn , ^{75}As , ^{85}Rb , ^{88}Sr , ^{107}Ag , ^{114}Cd , ^{138}Ba , ^{205}Tl , ^{208}Pb , ^{238}U . A correction equation ($\text{Pb208}=\text{Pb208}+\text{Pb206}+\text{Pb207}$) was used to determine Pb quantitatively. The analyses were carried out with the method of the internal standard (10 $\mu\text{g/L}$ solution of ^{103}Rh) introduced on-line with the peristaltic pump. All standards and solutions were prepared with the ultrapure deionized Milli-Q-Gradient water (Merck Millipore, Germany). A certified multi-element solution was used for calibration. It was prepared through diluting 10 mg/L of the calibration solution no. VI (Merck, Germany) and 1 g/L single element standards of Cd, Pb and Zn (Merck, Germany). A certified multi-element solution no. XXI (Merck, Germany) was applied to verify the calibration. All standards were prepared daily with the weight-to-weight dilution.

pH and electric conductivity were measured immediately after the samples were transported into the laboratory. The measurements were made with the multifunction meter CX-401 (Elmetron, Poland) in accordance with the standard [24, 25]. A soil suspension was prepared according to the Standard [26, 27] to determine soil pH and electric conductivity.

3. Results and discussion

3.1. Quality control

The aim of the analytical method validation was to decide whether the analysis process was conducted in a reliable way and the obtained results were trustworthy. The following analysis stages were validated: examination of the method accuracy and precision, determination of the detection and quantification limits, determination of the analyte recovery.

The standard definition for the detection limit in the XRF technique is that the net peak intensity should be three times higher than the standard deviation of the noise. In the research procedure, the number of

background counts was obtained through averaging background counts of 31 measurements of the control real sample. The quantification limits were determined as the product of a triple detection limit value (Table 2). The results from the background measurements obtained during the determination of the detection limits were used to establish the EDXRF method repeatability. Long-term measurements of the real material sample were performed to determine the intermediate precision (reproducibility) of the method. The measurements were made between December 2011 and January 2013.

Table 2. Validation parameters for the EDXRF methodology

Tabela 2. Parametry walidacyjne dla metody EDXRF

Analyte	Limit of detection [mg/kg]	Limit of quantification [mg/kg]	NIST 2709	Obtained average results [n=31]	Recovery [%]	Relative standard deviation of repeatability [%]	Relative standard deviation of reproducibility [%]
Al ₂ O ₃	94.78	284.34	14.17%	14.01%	98.86	37.4	12.8
SiO ₂	214.48	643.45	63.4%	56.1%	88.51	2.1	4.1
K ₂ O	8.63	25.89	2.45%	2.13%	87.15	2.4	12.4
CaO	13.19	39.56	2.64%	2.11%	79.97	3.5	5
TiO ₂	10.25	30.75	0.57%	0.52%	92.09	1.1	4.5
V	6.01	18.02	112 mg/kg	99.4 mg/kg	88.74	3.4	15.6
Cr	0.41	1.22	130 mg/kg	114 mg/kg	87.69	2.7	27.2
Mn	5.31	15.94	538 mg/kg	534 mg/kg	99.26	2	4.6
Fe ₂ O ₃	4.63	13.9	5.00%	4.65%	93.01	0.5	8.6
Ni	2.53	7.58	88 mg/kg	86 mg/kg	98.48	3.5	12.9
Cu	0.71	2.14	34.6 mg/kg	32.5 mg/kg	93.88	7.6	10.6
Zn	0.97	2.92	106 mg/kg	109 mg/kg	103.53	0.5	6.1
As	1.02	3.06	17.7 mg/kg	18.5 mg/kg	104.29	5.8	33.5
Rb	0.34	1.01		89.8 mg/kg		0.7	4.5
Sr	0.73	2.18	231 mg/kg	214 mg/kg	92.65	1	4.6
Zr	0.67	2		141 mg/kg		0.4	6.1
Mo	0.55	1.64		1.92 mg/kg		13.8	20.2
Cd	0.8	2.4		0.66 mg/kg		17.5	25.1
Sb	0.76	2.29		7.03 mg/kg		17.5	29
Cs	0.79	2.36		4.87 mg/kg		8	12.4
Ba	0.96	2.87		916 mg/kg		0.3	3.5
Pb	0.6	1.8	18.9 mg/kg	13.6 mg/kg	71.77	1.9	6.4
Y	1.05	3.14		16.9 mg/kg		1.5	4.7
Nb	0.89	2.68		10.3 mg/kg		2.5	4
Sn	1.02	3.07		1.48 mg/kg		4.3	9.9

For the ICP-MS, the detection limit was the product of a triple standard deviation for the blank sample ($n=31$). The blank was an acidified water sample used afterwards to prepare calibration and dilutions of all solutions and real samples (Table 3). The quantification limits were also determined as the product of a triple detection limit value. Multiple measurements ($n=31$) of the standard solution no. XXI (Merck, Germany) were performed to determine the repeatability of the ICP-MS method. Long-term measurements of this solution were made to determine the intermediate precision (reproducibility) of the method. The measurements were made between March 2011 and December 2012.

Table 3. Validation parameters for the ICP-MS methodology

Tabela 3. Parametry walidacyjne dla metody ICP-MS

Analyte	Limit of detection [$\mu\text{g/L}$]	Limit of quantification [$\mu\text{g/L}$]	NIST 1643-e [$\mu\text{g/L}$]	Obtained average results [$\mu\text{g/L}$] $n=31$	Recovery [%]	Relative standard deviation of repeatability [%]	Relative standard deviation of reproducibility [%]
Co	0.002	0.006	27	30	110	2.6	4.6
Ni	0.024	0.072	62	67	107	3.9	4.6
Cu	0.064	0.192	23	22	96	3.5	5.8
Zn	0.181	0.543	79	63	80	7.6	11.4
Cd	0.04	0.12	6.6	6.4	97	5.3	11.8
Pb	0.036	0.108	20	21	106	7.3	13.9
As	0.096	0.288	60	53	88	3.8	5
Cr	0.013	0.039	20	24	116	3.9	5.5
Mn	0.033	0.099	39	42	108	6.3	10.4
Ba	0.01	0.03	544	562	103	6.5	8.2
Rb	0.003	0.009	14	15	105	1.9	3.1
Sr	0.008	0.024	323	347	107	3.9	5.1
Ag	0.002	0.006	1.1	1.0	95	3.2	6.9
Tl	0.002	0.006	7.4	8.0	107	3.9	7.1
V	0.09	0.27	38	42	111	3.2	3.8

3.2. Metals and metalloids movements in groundwater

Metal pollution is a problem present in many contaminated areas. Pb, Cr, As, Zn, Cd, Cu and Hg are the most popular metals in the postindustrial areas. The presence of metals in soils and groundwater can pose a considerable threat for human health and ecological systems. Surface and underground water can be polluted with metals coming from

wastewater or discharges or through the direct contact with the polluted soil, slime, mine waste or debris [14]. The environmental impact of coal-mining wastes is determined by the characteristics of the extracted rock material, which can vary significantly, both horizontally and vertically through the coal-bearing Carboniferous strata. Table 4 presents results of quantitative analysis of the rock material of Hałda Ruda dump using EDXRF techniques. Table 5 presents standard deviations as well as minimum, maximum and mean values of the analyte concentrations in groundwater sampled from the piezometer network built up around the Hałda Ruda. Table 5 shows also some of the guidelines concerning the content of metals and metalloids in the waters [28, 34, 35].

Table 4. Results of quantitative analysis of the rock material of Hałda Ruda dump using EDXRF techniques

Tabela 4. Wyniki ilościowej analizy materiału skalnego zwału Hałda Ruda z wykorzystaniem techniki EDXRF

Analyte	Value	Unit
V	136	mg/kg
Cr	311	mg/kg
Mn	720	mg/kg
Fe ₂ O ₃	4.6	%
Co	25	mg/kg
Ni	85	mg/kg
Cu	86	mg/kg
Zn	750	mg/kg
As	8.1	mg/kg
Mo	3.2	mg/kg
Cd	14	mg/kg
Sb	7.3	mg/kg
Ba	647	mg/kg
Pb	172	mg/kg

Compared with the metals and metalloid guidelines in waters exceeding the highest content of toxic elements were found in water samples taken at runoff of the groundwater. Particularly elevated concentrations were observed in the case of lead, arsenic, chromium and zinc.

Table 5. International guidelines, standard deviations, minimum, maximum and mean contents of pH, conductivity the analyzed metals in water samples collected from piezometers no. P8–P9 (groundwater inflow) and P12 (groundwater runoff) between 2010 and 2012. Water samples measured using ICP-MS technique. LOD – Limit of Detection

Tabela 5. Międzynarodowe wytyczne, minimalne, maksymalne, średnie i odchylenie standardowe zawartości badanych metali/metaloidów w próbkach wód pobranych z piezometrów P8 i P9 (kierunek napływu wód gruntowych) oraz P12 (kierunek spływu wód gruntowych); próbki wód mierzone wykorzystując technikę ICP-MS. LOD – granica wykrywalności

Analyte	Piezometer P8 – Inflow				Piezometer P9 – Inflow				Piezometer P12 – Runoff				International guidelines			
	min.	max.	mean	SD	min.	max.	mean	SD	min.	max.	mean	SD	US EPA Drinking water	EU Drinking water	PL Ground water I class	
V [µg/L]	0.25	5.0	1.1	1.5	0.01	0.9	0.37	0.31	4.1	13	8.1	3.5			4	
Mn [µg/L]	7.2	479	221	182	198	662	363	152	1094	2337	1407	404	50	40	50	
Co [µg/L]	0.30	6.3	3.4	2.1	0.5	7.6	2.7	2.1	4.6	9.2	6.2	1.4		20	20	
Ni [µg/L]	3.9	10	5.5	2.0	4.3	13	10	2.5	14	22	17	2		20	5	
Cu [µg/L]	0.8	17	4.3	5.4	0.44	5.4	1.2	1.5	2.4	36	7.1	12	1300	2000	10	
Zn [µg/L]	6.9	30	18	7.8	3.7	46	1.5	12	14	236	50	76	5000		50	
As [µg/L]	0.39	3.5	1.6	1.0	0.6	3.0	1.6	1.0	7	15	10	2.6	6	5	10	
Rb [µg/L]	0.9	8.0	4.2	2.3	0.7	2.1	1.3	0.5	1.6	7.5	2.9	2.1				
Sr [µg/L]	116	573	182	147	148	221	188	26	1245	2144	1684	313				
Ag [µg/L]	0.02	0.8	0.25	0.26	0.01	0.09	0.05	0.03	0.01	1.5	0.42	0.5	100	50	1	
Cd [µg/L]	0.01	0.41	0.15	0.15	0.02	0.09	0.05	0.03	0.06	3.0	0.5	1.0	5	5	1	

Table 5. cont.
Tabela 5. cd.

Analyte	Piezometer P8 – Inflow			Piezometer P9 – Inflow			Piezometer P12 – Runoff				International guidelines				
	<i>min.</i>	<i>max.</i>	<i>mean</i>	<i>SD</i>	<i>min.</i>	<i>max.</i>	<i>mean</i>	<i>SD</i>	<i>min.</i>	<i>max.</i>	<i>mean</i>	<i>SD</i>	<i>US EPA Drinking water</i>	<i>EU Drinking water</i>	<i>PL Ground water I class</i>
Te [$\mu\text{g/L}$]	0.32	1.1	0.6	0.26	0.46	0.8	0.6	0.12	0.36	1.1	0.7	0.26			
Ba [$\mu\text{g/L}$]	26	84	47	19	40	73	53	11	35	79	53	15	2000		300
Tl [$\mu\text{g/L}$]	0.01	0.04	0.02	0.01	0.01	0.03	0.02	0.01	0.03	0.13	0.08	0.05	2		1
Pb [$\mu\text{g/L}$]	0.01	11	1.7	3.7	0.03	2.3	0.5	0.7	<LOD	132	17	47	15	10	10
Fe [$\mu\text{g/L}$]	480	4970	2514	167	277	3126	1373	1033	1147	11559	5282	4311	300	200	200
Cr [$\mu\text{g/L}$]	0.27	3.7	1.8	1.3	0.28	3.5	1.7	1.4	17	45	28	10	100	50	10
Bi [$\mu\text{g/L}$]	0.01	5.7	1.0	1.9	0.00	0.9	0.25	0.32	0.01	0.7	0.22	0.25			
Ga [$\mu\text{g/L}$]	1.5	3.2	2.2	0.5	1.2	3	3	0.7	1	3	2	0.7			
Mol [$\mu\text{g/L}$]	0.04	0.5	0.32	0.14	0.03	0.30	0.18	0.09	0.24	0.7	0.5	0.15			3
U [$\mu\text{g/L}$]	0.14	3.1	0.9	0.9	0.21	0.9	0.5	0.24	2.6	4.6	3.5	0.6	30		9
pH	6.45	6.99	6.87	0.19	6.45	7.08	6.56	0.22	6.88	7.02	6.92	0.06			
cond. [$\mu\text{s/cm}$]	325	458	414	56	482	565	519	35	5949	6218	6043	113			

Long-term storage of coal mine waste involves the risk that the pollutants may penetrate groundwater. When taking into consideration the groundwater inflow direction, it is visible that metal/metalloid concentrations were higher in the samples collected from the piezometers located on the groundwater runoff (P10, P11, P12).

Piezometers P10 and P11 during research were often dry. Therefore, in our considerations were taken into account the groundwater results obtained from P12 piezometer.

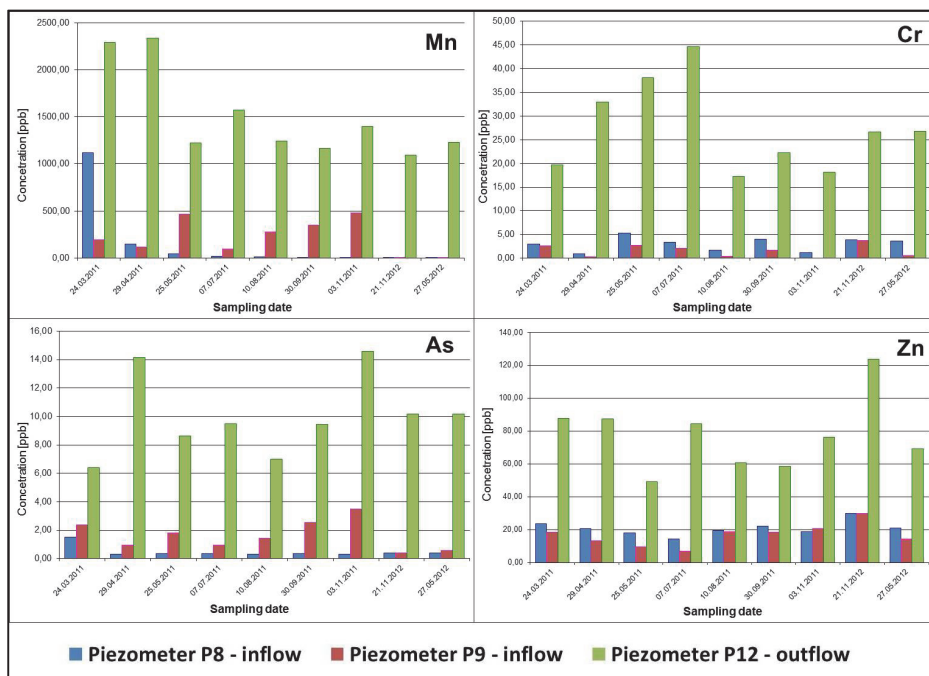


Fig. 2. Changes in concentrations of Mn, Cr, As and Zn in groundwater samples collected from the piezometers on the groundwater inflow (P8, P9) and runoff (P12)

Rys. 2. Zmiany w stężeniu Mn, Cr, As oraz Zn w próbkach wód gruntowych pobranych z piezometrów na napływie (P8 i P9) i spływie (P12)

Figure 2 shows the changes in the concentrations of Mn, Cr, As and Zn in groundwater samples collected from the piezometers on the water inflow and runoff. The parameters, together with the pH and electric conductivity values, show that the coal mine waste was the source of pollutants penetrating the surrounding environment. Moreover, the Bytomka

River flows in the groundwater runoff direction along the Hałda Ruda. The Bytomka River water and bottom sediments were polluted with the groundwater. The pollution was transferred into the Kłodnica River and from there into the Oder [17].

The electric conductivity of the groundwater samples collected on the water runoff (P12) was very high (approx. 6000 $\mu\text{S}/\text{cm}$). The data clearly shows that increased contents of chloride salts and sulfates were responsible for this situation (P8 on the groundwater inflow, $[\text{Cl}^-] = 20 \text{ mg/L}$ and $[\text{SO}_4^{2-}] = 286 \text{ mg/L}$; P9 on the groundwater inflow, $[\text{Cl}^-] = 39 \text{ mg/L}$ and $[\text{SO}_4^{2-}] = 72 \text{ mg/L}$; P12 on the groundwater runoff, $[\text{Cl}^-] = 1,167 \text{ mg/L}$ and $[\text{SO}_4^{2-}] = 703 \text{ mg/L}$). The salts were leached from the coal waste dump.

3.3. Metals and metalloids movements in the ground environment

Chemical and physical properties of a matrix (such as coal mine waste) polluted with metals influence the metal mobility in soils and groundwater. Pollutants in the soil matrix occur in three forms, i.e. pollutants solved in the soil moisture, pollutants adsorbed on the soil surface, and permanent soil pollutants. Chemical and physical soil properties influence the metal pollution form, its mobility and the selection of the area reclamation technology [17]. Table 8 presents international guidelines, maximum, minimum and mean metal/metalloid concentrations in the soil samples collected on the groundwater inflow and runoff. Around the Hałda Ruda, 24 boreholes were prepared in the network of 8 transects (Figure 1). The soil sampling points (boreholes) moved farther and farther away from the coal waste dump at each transect. The results were analyzed in numerous ways. The changes in the concentrations of selected metals and metalloids were investigated within each transect and genetic horizon. Research on metals and metalloids concentration in soils from surrounding the pile area compared with the soil quality guidelines (Table 6) clearly indicate that the areas situated at the confluence of ground water are more polluted with metals and their number many times exceed those limits. Concentration of lead in the soil even exceeded 2000 mg/kg. In the case of copper, manganese, chromium or zinc huge exceeded permissible levels were also observed.

Additionally, chemometric analysis with the concept of dissimilarity [40] and principal component analysis (PCA) [1, 19, 37, 41] were carried out.

Table 6. International guidelines, maximum, minimum and average contents and standard deviation of the measured elements in the soil samples in transects located on the groundwater inflow and runoff. Soil samples measured using EDXRF technique

Tabela 6. Międzynarodowe wytyczne, maksymalne, minimalne, średnie i odchylenie standardowe mierzonych pierwiastków w próbkach gleb pobranych w transektach rozmieszczonych po stronie napływu i spływu wód gruntowych. Probki gleb mierzono przy użyciu techniki EDXRF

Analyte	Unit	Inflow – Transects 1. 2. 3. 7. 8 (n=58)				Runoff – Transects 4. 5. 6 (n=58)				International guidelines			
		min.	max.	mean	SD	min.	max.	mean	SD	EPA	EU	PL A Class	
V	mg/kg	21	115	54	22	20	292	66	51	90	50		
Cr	mg/kg	23	287	102	61	5.1	1.207.60	170	219	70	40	50	
Mn	mg/kg	130	671	283	112	1.0	2.675.90	330	447				
Fe ₂ O ₃	%	1.1	4.3	2.5	0.8	0.33	13	3.2	2.3				
Co	mg/kg	<LOD	24	6.3	5.6	<LOD	46	10	9.2	20	20	20	
Ni	mg/kg	7.5	79	24	16	0.71	159	29	30	40	40	35	
Cu	mg/kg	<LOD	85	19	20	<LOD	2.048.50	177	381	60	40	30	
Zn	mg/kg	15	695	159	162	1	9.675.30	788	1.862.20	300	150	100	
As	mg/kg	1.0	7.9	4.0	1.5	0.61	42	7.4	10	10	10	20	
Mo	mg/kg	0.04	3	1.0	0.6	<LOD	10	1.8	1.9			10	
Cd	mg/kg	0.37	13	1.4	2.1	0.24	59	4.9	11	1	1	1	
Sb	mg/kg	0.31	6	1.0	0.9	0.31	698	91	174	1	1		
Ba	mg/kg	107	584	295	110	5.8	1.057.40	305	215	200	300	200	
Pb	mg/kg	5.6	164	38	43	1.4	2.185.00	161	382	45	40	50	
Sn	mg/kg	1.4	6.6	3.0	1.0	1.6	292	34	62	5	1		
pH	-	5.43	8.71	6.75	0.86	6.31	8.94	7.31	1.11				
cond.	[µs/cm]	11	526	96	109	40	526	177	105				

To perform the soil type imaging, agricultural maps were used and several reconnaissance soil pits were prepared. The soils of the corresponding type, structural group and thickness were compared. The obtained data enabled specific comparisons within the entire transect. Table 1 presents the distances of particular sampling points from the coal waste dump. Transects I, II, III were placed on the groundwater inflow whereas transects IV, V, VI were located on the groundwater runoff (Figure 1). Transects VII and VIII were selected due to their close location to the houses in Trębacka Street. Transect I was placed on the groundwater inflow. The metal/metalloid mobility along the transect depended on the metal/metalloid. The Cd concentration, similarly to Pb, was high in the upper soil layers. It could be the result of the winds blowing in this area (S-W). The concentrations of the above-mentioned metals were lower in the deeper genetic horizons. Within a profile, the concentrations decreased with the growing distance from the coal waste dump. The Cr concentration, dwindling with the growing distance from the coal waste dump, was the most visible example of the metal mobility.

The Zn and Co concentrations decreased at the 100 m distance from the coal waste dump and then increased. Importantly, the large Zn content was found in the upper soil layer (0–30 cm). The increase in the Zn concentration could have been caused by the location of the rails close to Point 3 in Transect I.

Transect II, lying close to Transect I, was also placed on the groundwater inflow. The concentrations of Cd, Zn, Cu and Pb decreased dramatically in the upper layer (0–30 cm) with the growing distance from the coal waste dump. The differences at deeper genetic horizons were slight. Such a situation seems to have been influenced by the deposition of the dust from the coal waste dump. Moreover, the water running off from the dump slope polluted the areas lying close to the coal waste dump to a larger extent. Similarly to Transect I, the Cr concentration was strongly correlated with the sampling point distance from the coal waste dump. It was independent of the genetic horizon from which the sample had been collected. Interestingly, the Sb results indicate that its concentration rose at a larger distance from the coal waste dump. It could be related to the material deposition in the form of dust from which the dump had been built. Moreover, the western part of the coal waste dump was not tree-covered and constituted a significant source of such pollu-

tants. For Ni, the decrease in its concentration was observed in the deeper soil layers and with the growing distance from the waste dump. The upper soil layer became enriched with Ni when the distance rose. It could be related to the dusting from the coal waste dump and transporting the metals on the smallest particles.

The Zn concentration decreased in Transect III when the distance from the coal waste dump rose. Its increased concentration was observed in the upper soil layer. The results indicate the profound influence of the waste from the dump on the Zn concentration in the soil surrounding the dump. The Ni, As, Cr and Cd concentrations decreased dramatically in the upper soil layers with the growing distance from the coal waste dump. When comparing metal concentrations in the soil samples collected at Transect IV, typical correlations between their decrease and the growing distance from the coal waste dump were observed. Transect V was located on the groundwater runoff in the north-west part of the Hałda Ruda, close to the Bytomka River. The Cd, Pb and As concentrations fell when the distance from the coal waste dump rose. There were large differences in concentrations between various genetic horizons. The Cr and Ni concentrations decreased with the growing distance from the coal waste dump. Nevertheless, the differences observed between various genetic horizons were much slighter. Interestingly, V, Mn, Fe, Co and Ba constituted an element group of similar mobility. The concentration charts of these elements indicate similar concentrations at Points 1 and 3. They were higher at Point 2. It was probably related to the additional impact of the municipal pollution from Biskupice, one of Zabrze's districts. For Transect VI, concentrations of most elements decreased with the growing distance from the coal waste dump. The variations in the Cr, As, Ni, Pb, Cu and Zn concentrations revealed similarities. The Hałda Ruda is partially planted with trees and partially uncovered. When taking into account the direction of the dominant winds (S-W), the increase in metal concentrations in the upper soil layer of Transect VI (northern slope) was observed. Most winds blew in this direction. They transported the waste material deposited at the coal waste dump in the form of dust (Figure 3). The process had a strong impact on the movement of pollutants.

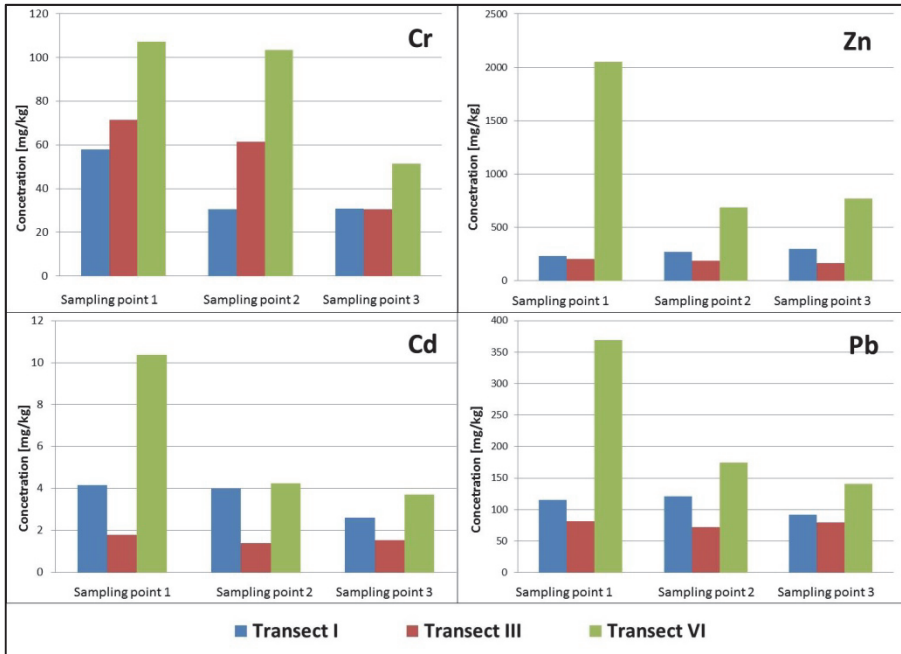


Fig. 3. Impact of the dominant winds on the increase in the Cr, Zn, Cd and Pb concentrations in the upper soil layers of the areas surrounding the Hałda Ruda
Rys. 3. Wpływ dominujących wiatrów na wzrost stężenia Cr, Zn, Cd oraz Pb w wierzchnich warstwach gleby terenu otaczającego zwał Hałda Ruda

Figure 4 shows total concentrations of Mn, Zn, Pb and Cu in 2 profiles of the polluted soil collected from the sampling points located at Transects II and VI. Significant differences in the Pb, Cu, Zn and Mn concentrations depended on the depth. It was particularly visible in the highest concentration of these metals observed in the upper soil layer collected at Point 1 of Transect VI (Figure 4A). These findings prove that the secondary deposition and runoff water were the main sources of the soil pollution. On the other hand, the differences in the concentrations of Pb, Zn, Mn and Cu in the soil profile were much lower at Point 1 of Transect II. They resulted from the location of Transect II on the groundwater inflow. The dominant winds influenced the secondary deposition of the waste material (Figure 4B) to a lesser extent.

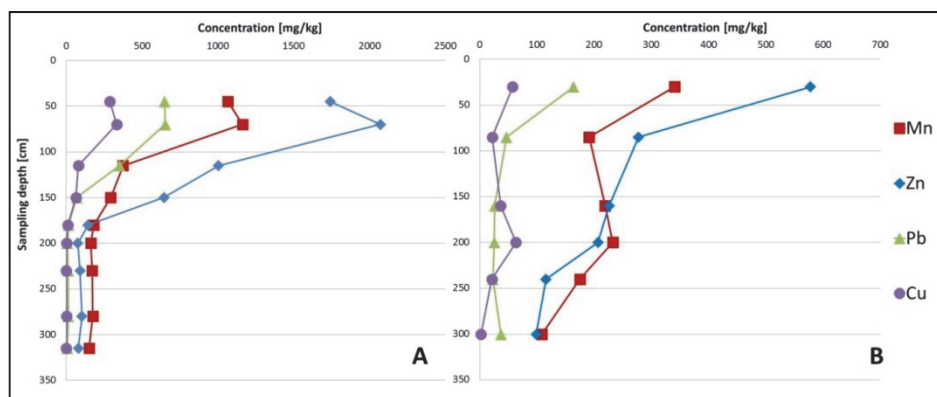


Fig. 4. Changes in total concentrations of Mn, Zn, Pb and Cu in the soil profiles collected at **A)** Point 1, Transect VI (groundwater runoff) **B)** Point 1, Transect II (groundwater inflow)

Rys. 4. Zmiany stężenia całkowitego Mn, Zn, Pb oraz Cu w profilach glebowych pobranych **A)** w Punkcie 1 Transekt VI (kierunek spływu wód gruntowych) **B)** w Punkcie 1 Transekt II (kierunek napływu wód gruntowych)

Trębacka Street, where the houses are located, lies close to the Hałda Ruda. For that reason, soil samples from Transects VII and VIII were collected at this side of the coal waste dump. The soil in this area mainly contains loam and clay. This might have been one of the reasons for building houses there despite the close location of the coal waste dump. Metal concentrations in the upper soil layer collected at these transects were much higher than those observed at lower horizons. This was probably caused by the process of the upper layer enrichment with metals originating from the runoff water. Metal concentrations decreased when the distance from the waste dump rose. As the eastern part of the Hałda Ruda was planted with trees, no influence of the dust transportation was observed. The tree cover constituted an important barrier that isolated the houses in Trębacka Street from the Hałda Ruda.

3.3. Chemometric analysis

3.3.1. Preprocessing and dissimilarity analysis

The measurement data concerning pH, electrical conductivity and contents of selected chemical substances in the soil samples collected at 8 transects were organized in the matrix **X** of 114 objects (samples) and

17 parameters. The data preprocessing embraced it centering and standardization in accordance with the dependence:

$$x_{ij,a} = \frac{(x_{ij} - \bar{x}_j)}{s_j} \tag{1}$$

where:

\bar{x}_j – arithmetic mean of the j -th column;

s_j – standard deviation of the j -th parameter;

x_{ij} and $x_{ij,a}$ – i -th value of the j parameter before and after autoscaling, respectively.

After the preprocessing, the data underwent visualization through calculating the dissimilarity matrix **D** (dimensions: 114 x 114) with the Euclidean distance as the measure of dissimilarity [40]. The calculations were made according to the formula of Al-Kashi (Persian mathematician from the 15th century), whose matrix form was [41]:

$$\mathbf{D}^2 = \left(\text{diag}(\mathbf{XX}^T) \cdot \mathbf{1}^T + \mathbf{1} \cdot \text{diag}(\mathbf{XX}^T)^T \right) - 2 \cdot (\mathbf{XX}^T) \tag{2}$$

where:

$\mathbf{1}^T$ – row vector of 114 elements equal to 1;

$\mathbf{1} \cdot \text{diag}$ – an operator extracting only the diagonal elements from the matrix represented as a column vector.

To obtain matrix **D**, the root of the matrix **D**² value, calculated according to the formula (2), had to be calculated.

The determined dissimilarity matrix (Figure 5) helped to examine the data structure and observe the highest diversification of the objects in Transects IV and VI. The observation was corroborated when the average distance of a given object from other ones was determined (Figure 6).

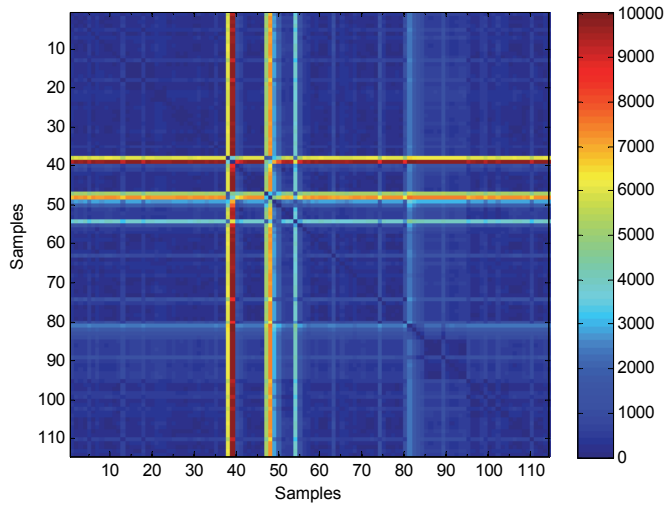


Fig. 5. Dissimilarity matrix D calculated with the Euclidean distance
Rys. 5. Macierz podobieństwa D obliczona z wykorzystaniem odległości Euklidesa

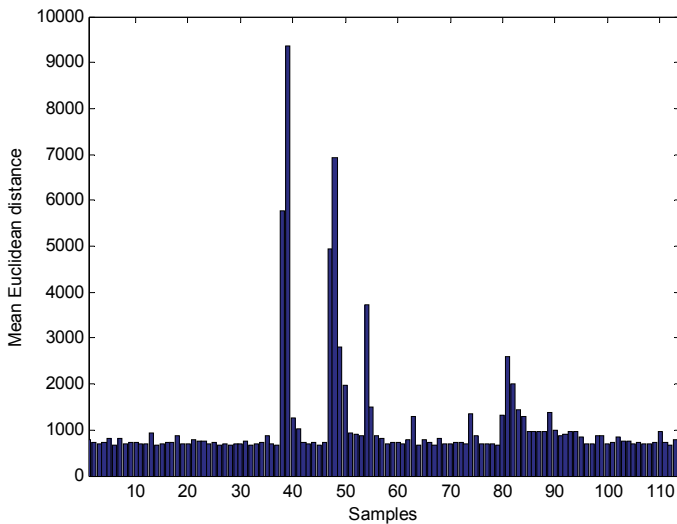


Fig. 6. Detection of distant objects with dissimilarity matrix D
Rys. 6. Detekcja obiektów odległych z wykorzystaniem macierzy podobieństwa D

The most distinctive objects were: object 39 (Point 1, Transect IV, thickness: 45–70 cm), object 48 (Point 2, Transect IV, thickness: 45–50 cm), object 38 (Point 1, Transect IV, thickness: 0–45 cm), object 47 (Point 2, Transect IV, thickness: 0–45 cm) and object 54 (Point 3, Transect IV, thickness: 0–40 cm). It is probably related to the fact that the sampling points of Transect IV were placed in the inundation area of the Bytomka River. The river overflows the banks every year during the spring thaw and covers the upper soil layer with sediments and alluvia. Soil layers characteristic for such areas (silt, peat) were found at the depth of up to 4 m, which meant that the Bytomka River had been overflowing the banks at this area for many years.

3.3.2. Principal component analysis

Principal Component Analysis (PCA) [1, 19, 37, 41] allows investigating the correlations between the measured parameters (contents of selected chemical substances and physicochemical parameters) and specific objects (samples). The algorithm of the Singular Value Decomposition (SVD) was used in the PCA. Firstly, the percentage of variance described by each principal component (PC) was calculated. The PC1, PC2 and PC3 accounted for 37.36%, 26.21% and 8.38% of variance, respectively. Further data analysis was performed for the first three components, which explained over 70% of the data variance. The correlations between 114 objects are visualized in Figure 7, which presents the projection of the objects onto the planes of PC1, PC2 and PC1, PC3.

The analysis of the PC1, PC2 (Figure 3a) and PC1, PC3 (Figure 3b) projections demonstrate that objects belonging to Transects IV and VI largely contributed to the PC1 and PC2, which proves the conclusions drawn from the dissimilarity matrix analysis. The greatest contributions to the creation of the third principal component (PC3) are the objects belonging to Transect VI. The soil samples from Transects IV and VI were the source of the greatest variance in the analyzed data set. The location in the inundation area of the Bytomka River was the main reason for the variety in Transect IV. On the other hand, the dominant direction of the blowing winds and municipal pollution were the sources of the largest variance in Transect VI. The correlations between the analyzed parameters are shown in the charts of loadings (Figure 8).

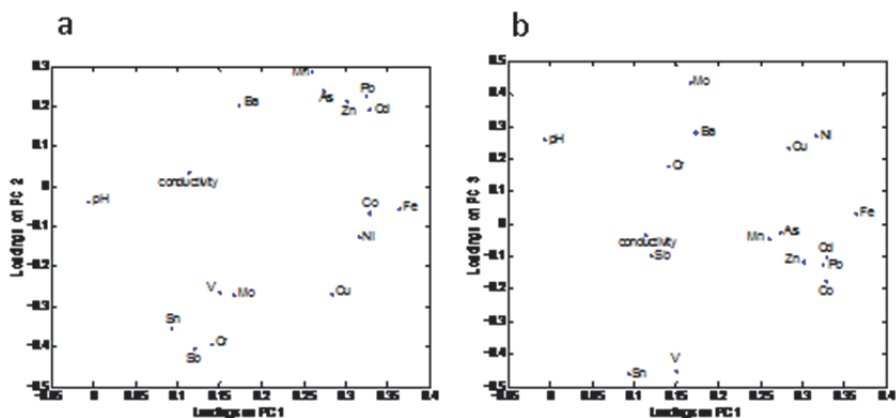


Fig. 7. Projection of objects onto the plane: a) PC1, PC2; b) PC1, PC3

Rys. 7. Projektcja obiektów na płaszczyznę: a) PC1, PC2; b) PC1, PC3

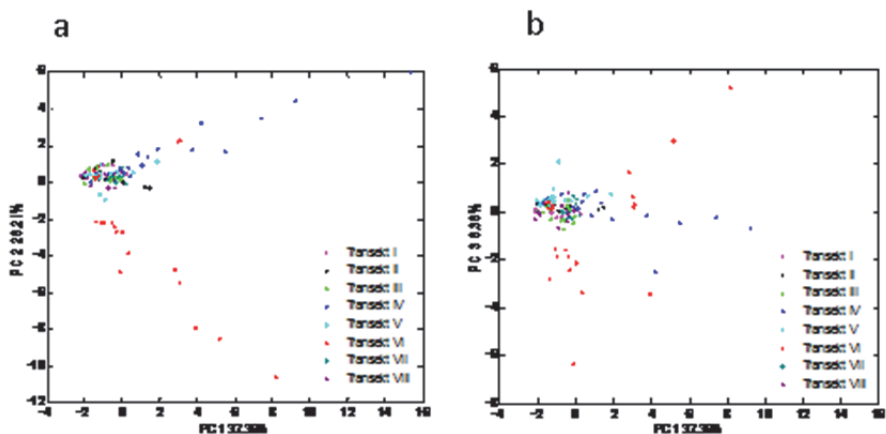


Fig. 8. Projection of charges onto the plane: a) PC1, PC2; b) PC1, PC3

Rys. 8. Projektcja ładunków na płaszczyznę: a) PC1, PC2; b) PC1, PC3

The projection of loadings onto the PC1, PC2 plane indicated a strong positive correlation between the contents of elements and chemical compounds within 3 groups. The first group was made by Ba, Mn, As, Pb, Zn and Cd. Co, Ni and Fe₂O₃ belonged to the second group. The third one contained Sn, Sb, Cr, Mo and V. Chart 4a also points to the lack of correlations between the elements from the first and third groups. The

projection of loadings onto the PC1, PC3 plane confirms most conclusions from the Figure 4a analysis. An in-depth analysis of Figure 4 provides information on the parameters differentiating soil samples that belong to Transects IV and VI from other samples. The parameters included the contents of Fe_2O_3 , Sb, Sn, Cr, V and Mo.

4. Conclusions

The research conducted at the Hałda Ruda clearly demonstrates that even old and no longer used coal waste dumps still pose a threat to the environment. They influence increases in the contents of heavy metals accumulating in the surrounding water and soil environment. The Hałda Ruda is relatively old in comparison with other coal waste dumps in the Upper Silesia urban area. Nonetheless, large amounts of chlorides and sulfates are leached from it with runoff and groundwater. Consequently, the Hałda Ruda is still the source of metals and metalloids leached from the waste dump. The pollution of the soil environment with metals/metalloids leaching from the deposited waste is higher on the groundwater runoff and in the area influenced by the dominant winds.

The chemometric analysis allowed to find transects with the largest degree of object diversification (Transects IV and VI). The findings were confirmed with the field research. The PCA corroborated the existence of a ceratin element group (Mn, As, Zn, Pb, Cd). The elements were characterized by the strong correlation between their contents in the soil samples. They were leached from the waste deposited at the coal waste dump (together with chlorides and sulfates) with groundwater.

Using the coupled EDXRF and ICP-MS spectrometers turned out to be the best solution allowing for the measurements of water and soil samples at different concentration levels.

The work is the result of a grant no. NN 523 42 15 37.

Abbreviations used in text:

EDXRF – Energy Dispersive X-Ray Fluorescence,

ICP-MS – Inductively Coupled Plasma Mass Spectrometry,

PCA – Principal Component Analysis,

CA – Cluster Analysis,

XRF – X-Ray Fluorescence,

AMSL – Above Mean Sea Level,

cond. – Conductivity,
LOD – Limit of Detection.

References

1. **Abdi H., Williams L. J.:** *Principal component analysis. WIREs Computational Statistics*, 2, 433–447 (2010).
2. **Akyuz S., Akyuz T., Algan A. O., Mukhamedshina N. M., Mirsatogova A. A.:** *Energy dispersive X-ray fluorescence and neutron activation analysis of surficial sediments of the Sea of Marmara and the Black Sea around Istanbul. Journal of Radioanalytical and Nuclear Chemistry*, 254, 569–575 (2002).
3. **Aleksander-Kwaterczak U., Ciszewski D.:** *Groundwater hydrochemistry and soil pollution in a catchment affected by an abandoned lead–zinc mine: functioning of a diffuse pollution source. Environmental Earth Sciences*, 65, 1179–1189 (2012).
4. **Aleksander-Kwaterczak U., Helios-Rybicka E.:** *Contaminated sediments as a potential source of Zn, Pb, and Cd for a river system in the historical metalliferous ore mining and smelting industry area of South Poland. Journal of Soils and Sediments*, 9, 13–22 (2009).
5. **Astel A., Głosińska G., Sobczyński T., Boszke L., Simeonov V., Siepak J.:** *Chemometrics in the assessment of the sustainable development rule implementation. Central European Journal of Chemistry*, 4, 543–564 (2006).
6. **Benvenuti M., Mascaro I., Corsini F., Lattanzi P., Parrini P., Tanelli G.:** *Mine waste dumps and heavy metal pollution in abandoned mining district of Boccheggiano (Southern Tuscany, Italy). Environmental Geology*, 30, 238–243 (1997).
7. **Bi X., Feng X., Yang Y., Qiu G., Li G., Li F.:** *Environmental contamination of heavy metals from zinc smelting areas in Hezhang County, western Guizhou, China. Environment International*, 32, 7, 883–890 (2006).
8. **Boyle J. F.:** *Rapid elemental analysis of sediment samples by isotope source XRF. Journal of Paleolimnology*, 23, 213–218 (2000).
9. **Cakir C., Budak G., Karabulut A., Sahin Y.:** *Analysis of trace elements in different three region coals in Erzurum (Turkey): a study using EDXRF. Journal of Quantitative Spectroscopy & Radiative Transfer*, 76, 101–106 (2003).
10. **Dang Z., Liu C., Haigh M. J.:** *Mobility of heavy metals associated with the natural weathering of coal mine spoils. Environmental Pollution*, 118, 419–426 (2002).
11. **Dinelli E., Tateo F.:** *Factors controlling heavy-metal dispersion in mining areas: the case of Vigonzano (northern Italy), Fe–Cu sulfide deposit associated with ophiolitic rocks. Environmental Geology*, 40, 1138–1150 (2001).

12. **Dos Anjos M. J., Lopes R. T., Assis J. T., Cesareo R., Barradas C. A. A.:** *Quantitative analysis of metals in soil using X-ray fluorescence*. Spectrochimica Acta Part B: Atomic Spectroscopy, 55, 1189–1194 (2000).
13. EU report from the commission to the European Parliament, the Council, the European Economic and Social Committee and the Committee of the Regions. The implementation of the Soil Thematic Strategy and ongoing activities
14. **Evanco C. R., Dzombak D. A.:** *Remediation of Metals Contaminated Soils and Groundwater*, Pittsburgh, USA, TE-97-01 Technology Evaluation Report, 1997.
15. **Frankowski M., Ziola-Frankowska A., Kurzyca I., Novotný K., Vaculovic T., Kanický:** *Determination of aluminium in groundwater samples by GFAAS, ICPAES, ICPMS and modelling of inorganic aluminium complexes*. Environmental Monitoring and Assessment, 182, 71–84 (2011).
16. **Henriques F. S.:** *Heavy Metal Content of Spoil Heaps from an Abandoned Iron- and Copper-Mine and Metal Accumulation in Armeria linkiana Nieto Feliner*. Bulletin of Environmental Contamination and Toxicology, 68, 555–560 (2002).
17. **Jabłońska-Czapla M., Szopa S., Rosik-Dulewska Cz.:** *Impact of mining dump on the accumulation and mobility of metals in the Bytomka River sediments*. Archives of Environmental Protection, 40, 2, 3–19 (2014).
18. **Jha S. K., Chavan S. B., Pandit G. G., Negi B. S., Sadasivan S.:** *Fluxes of Trace and Toxic Elements in Creek Sediment Near Mumbai, India*. Environmental Monitoring and Assessment, 76, 249–262 (2002).
19. **Jolliffe I.T.:** Principal Component Analysis, New York, Springer-Verlag
20. **Jorgensen N., Laursen J., Viksna A., Pind N., Holm P. E.:** (2005). *Multi-elemental EDXRF mapping of polluted soil from former horticultural land*. Environment International, 31, 43–52 (2002).
21. **Lewinska-Preis L., Jablonska M., Fabianska M. J., Kita A.:** *Bioelements and mineral matter in human livers from the highly industrialized region of the Upper Silesia Coal Basin (Poland)*. Environmental Geochemistry and Health, 33, 595–611 (2011).
22. **Mahmoud H. M., Abbady A. G. E., Khairy M. A., Abdehalim A. S., El-Taher A.:** *Multi-element determination in sandstone rock by instrumental neutron activation analysis*. Journal of Radioanalytical and Nuclear Chemistry, 264, 715–718 (2005).
23. **Marguí E., Padilla R., Hidalgo M. Queralt, I. Van Grieken R.:** *High-energy polarized-beam EDXRF for trace metal analysis of vegetation samples in environmental studies*. X-Ray Spectrometry, 35, 169–175 (2006).
24. PN-90-C-04540/01: 1990 – Water and wastewater – pH, acidity and alkalinity tests – Determination of pH of water and wastewater with a conductivity of 10 $\mu\text{S}/\text{cm}$ and above.

25. PN-EN 27888:1999 – Water quality – Determination of electrical conductivity.
26. PN-ISO 10390:1997 – Soil quality – Determination of pH.
27. PN-ISO 11265:1997 – Soil quality – Determination of electrical conductivity.
28. Regulation of the Minister of Health on 23 July 2008, about ground water quality, No. 143 pos. 896th.
29. Regulation of the Minister of Environment on 9 September 2002. Standards on soil quality, No. 165 pos. 1359.
30. **Skorek R., Jabłońska M., Polowniak M., Kita A., Janoska P., Buhl F.:** *Application of ICP-MS and various computational methods for drinking water quality assessment from the Silesian District (Southern Poland)*. Central European Journal of Chemistry, 10(1), 71–84 (2012).
31. **Sojka M., Siepak M., Ziola A., Frankowski M., Murat-Błażejewska S., Siepak J.:** *Application of multivariate statistical techniques for evaluation water quality of the Mała Welná river catchment, (WEST POLAND)*. Environmental Monitoring and Assessment, 147, 159–170 (2008).
32. **Szczepanska J., Twardowska I.:** *Distribution and environmental impact of coal-mining wastes in Upper Silesia, Poland*. Environmental Geology, 38, 249–258 (1999).
33. US EPA Ecological Soil Screening Level (Eco-SSL) Guidance and Documents <http://www.epa.gov/oerrpage/superfund/programs/risk/ecorisk/ecossl.htm>.
34. US EPA The Safe Drinking Water Act (SDWA), Pub. L. 93-523, 88 Stat. 1660 (1974).
35. EU Council Directive 98/83/EC of 3 November 1998 on the quality of water intended for human consumption.
36. **Walna B., Siepak K., Drzymala S.:** *Soil degradation in the Wielkopolski National Park (Poland) as an effect of acid rain simulation*. Water, Air, and Soil Pollution, 130, 1727–1732 (2001).
37. **Wold S., Esbensen K., Geladi P.:** *Principal Component Analysis*. Chemometrics and Intelligent Laboratory Systems, 2, 37–52 (1987).
38. **Yu K. N., Yeung Z., Lee L., Stokes M. J., Kwok R.:** *Determination of multi-element profiles of soil using energy dispersive X-ray fluorescence (EDXRF)*. Applied Radiation and Isotopes, 57, 279–286 (2002).
39. **Zhan X.:** *Application of polarized EDXRF in geochemical sample analysis and comparison with WDXRF*. X-Ray Spectrometry, 34, 207–211 (2005).
40. **Zerzucha P., Walczak B.:** *Concept of (dis)similarity in data analysis*. Trends in Analytical Chemistry, 38, 116–128 (2012).
41. **Zerzucha P., Boguszewska D., Zagdańska B., Walczak B.:** *Non-parametric multivariate analysis of variance in proteomic response of potato to the drought stress*. Analytica Chimica Acta, 719, 1–7 (2012).

Badania nad przemieszczaniem się metali i metaloidów w glebie i wodzie gruntowej terenów otaczających zwał odpadów pogórnich Hałda Ruda, Górny Śląsk, Polska

Streszczenie

Górny Śląsk to najbardziej przekształcone w wyniku działalności człowieka terytorium Polski. Celem pracy była optymalizacja i walidacja ilościowego oznaczania metali i metaloidów przy użyciu techniki EDXRF i ICP-MS do identyfikacji zanieczyszczeń na obszarach wokół składowiska odpadów pogórnich, Hałda Ruda (Zabrze, Polska Południowa) oraz określenie sposobu, w jaki metale i niemetale przenoszą się w glebach i wodach gruntowych na omawianym obszarze. Stężenia 27 metali i metaloidów oznaczano w próbkach gleb za pomocą techniki EDXRF. Próbkę wód gruntowych pobierano comiesięcznie między 2010 i 2012 i analizowano techniką ICP-MS. Uzyskane wyniki badań poddano analizie chemometrycznej, co pozwoliło na znalezienie transektów z największym stopniem dywersyfikacji obiektu. Analiza PCA potwierdziła istnienie pewnej grupy pierwiastków charakteryzujących się silną korelacją pomiędzy ich zawartością w próbkach gleb. Hałda Ruda nadal jest źródłem zanieczyszczeń w środowisku wodnogruntowym, szczególnie na terenach leżących w kierunku spływu wód gruntowych oraz w obszarze pod wpływem dominujących wiatrów południowo-zachodnich. W próbkach wód pobieranych na spływie wód gruntowych stwierdzono najwyższe stężenia toksycznych metali przekraczające dopuszczalne normy. Szczególnie podwyższone stężenie obserwowano w przypadku ołowiu, arsenu, chromu i cynku. Badania stężenia metali i metaloidów w glebach z obszarów otaczających teren zwału, w porównaniu z wytycznymi jakości gleb, jasno wskazują, że tereny usytuowane na spływie wód gruntowych są znacznie bardziej zanieczyszczone, a ich wartości wielokrotnie przekraczają dopuszczalne normy. Stężenie ołowiu w glebie przekraczało nawet 2000 mg/kg. Zaobserwowano również ogromne przekroczenia poziomu dopuszczalnego stężenia miedzi, manganu, chromu lub cynku. Maksymalne stężenia Cu, Zn, Pb lub Cr w wierzchnich warstwach gleby przekraczały kilka tysięcy mg/kg.

Słowa kluczowe:

ICP-MS, EDXRF, gleba, wody gruntowe, metale ciężkie, analiza chemometryczna, PCA

Keywords:

ICP-MS, EDXRF, soil, groundwater, heavy metals, chemometric analysis, PCA